PROCEEDINGS OF THE 10TH SYMPOSIUM ON THE GEOLOGY OF THE BAHAMAS AND OTHER CARBONATE REGIONS

Edited by
Benjamin J. Greenstein and Cindy K. Carney

Production Editor:
Dana Bishop

Gerace Research Center
San Salvador, Bahamas
2001

Front Cover: The reef crest indicator species, *Acropora palmata*, on Gaulin's Reef, San Salvador Island. Gaulin's Reef is a classic bank-barrier reef that has shown remarkable resilience following two significant disturbances: El Niño-induced warming of the sea surface in 1998 and Hurricane Floyd in September, 1999 (see Peckol et al., this volume). Photo by Janet Lauroesch.

Back Cover: The oolite shoals of Joulter's Cay, north of Andros Island, Bahamas, site of the pre-meeting field trip. Photo by Ben Greenstein.

ISBN 0-935909-69-9

THE SURFICIAL GEOLOGY OF THE HARD BARGAIN AREA, SAN SALVADOR ISLAND, BAHAMAS

Summer D. Sparkman-Johnson
Department of Geosciences
Mississippi State University
Mississippi State, MS 39762

James L. Carew
Department of Geology
College of Charleston
Charleston, SC 29424

John E. Mylroie
Department of Geosciences
Mississippi State University
Mississippi State, MS 39762

ABSTRACT

The Hard Bargain area of San Salvador Island, Bahamas offers a rich source of petrologic data, yet due to its rugged terrain and dense vegetation, accessibility into this region has been limited. Only now, with trail development, has this region been traversed and sampled. Prior to this study, surficial geology has been largely interpreted from samples collected from the perimeter of the island or from stratigraphic relationships observed at rock quarries, road-cuts, or other more readily accessible locations.

The geological models previously suggested for the geology of San Salvador Island by Titus (1980, 1987), Carew and Mylroie (1985, 1995, 1997), and Hearty and Kindler (1991, 1992, 1993) show an evident lack of agreement about some aspects of the geological history of the island. None of these models adequately addressed the large interior area called the Hard Bargain region.

Petrologic analyses of the rocks from the Hard Bargain region show a definite pattern of allochem distribution. The down-wind sides (or lee sides) of the ridges are composed predominantly of bioclasts, whereas the up-wind sides are predominantly oolitic. These observations suggest that older peloidal/bioclastic dunes (Owl's Hole Formation) appear to be partially mantled by a younger oolitic unit, the Grotto Beach Formation. The Grotto Beach Formation was deposited during oxygen-isotope substage 5e (~125 ka) and the Owl's Hole Formation was deposited during oxygen-isotope stage 7 and/or 9 (220 ka and/or 320 ka). The direction from which the younger oolitic deposits mantle the older peloidal/bioclastic deposits implies that wind asymmetry was a dominant factor in the depositional patterns observed.

These findings are consistent with Carew and Mylroie (1995, 1997), who suggested that these eolianite ridges represent two stratigraphic units, not one, as proposed by Hearty and Kindler (1993). Therefore, detailed sampling of the Hard Bargain region of San Salvador Island has provided a better understanding of the surficial geology of the island, and the stratigraphy and Quaternary history of the Bahamas.

INTRODUCTION

The geology of San Salvador Island, Bahamas has been studied extensively along coastal cliffs, road-cuts, and quarries, as these areas are convenient for investigation. However, the deep interior of the island, especially the interior of the Hard Bargain landmass (Figure 1), located between Long Lake (the name given to the northerly arm of Great Lake) on the west and Storr's Lake on the east, was almost entirely unknown from a geological perspective. This interior region is one of the largest on the island, and being covered by dense vegetation, is extremely inaccessible. The region consists of eolianite ridges and intervening swales with superimposed karst features such as banana holes and pit caves.

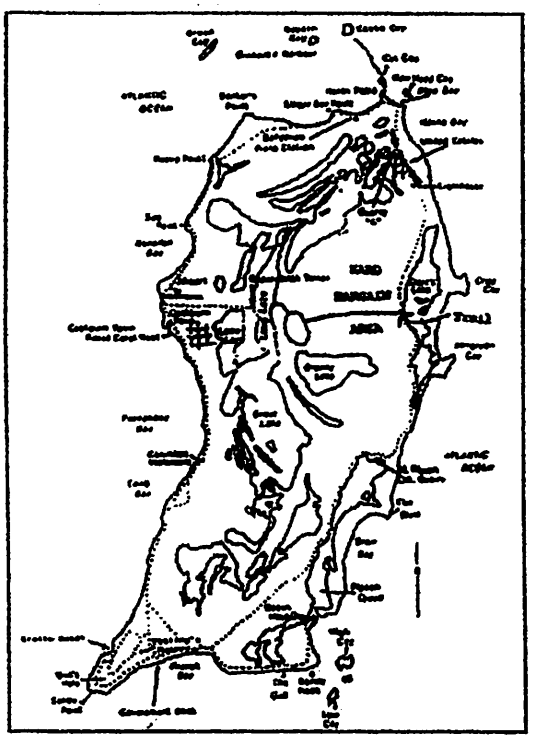

Figure 1. Map of San Salvador Island, with the Hard Bargain Trail labeled. 0.05 in. = 2750 m/1.7 mi.

The geological models suggested for the geology of San Salvador include those of Titus (1980, 1987), Carew and Mylroie (1985, 1995, 1997), and Hearty and Kindler (1991, 1992, 1993). These models offer slightly different interpretations of the geology of San Salvador, but none of them adequately addresses this interior region. The purpose of this investigation is to conduct a petrologic analysis of the Hard Bargain landmass in order to determine how it fits into current stratigraphic models.

METHODS

Samples were collected from outcrops on the flanks of the ridges and in karst features that are on, or adjacent to, a 5.4 km trail that was cut east-west through the Hard Bargain region. Samples were obtained by rock hammer or by taking cores using a rock drill. The resulting petrologic analysis provides a more accurate interpretation of the surficial geology of this region of San Salvador Island.

Sixty thin sections were prepared, and then examined using a petrographic microscope. Macroscopic observation with a hand lens was conducted on those samples that were too friable to survive thin section preparation. The thin sections were point counted and described by grain constituents and their relative percentages, grain-sizes, cement types and fabrics, porosity types, and the presence of other constituents such as root structures.

OBSERVATIONS

The Hard Bargain Trail starts just west of Storr's Lake on the eastern perimeter of the island, runs generally westward through the interior, and ends just east of Long Lake. The

trail traverses two main types of topographic features, linear to arcuate ridges and intervening swales. The main features observed from east to west are: 1) an 18 m ridge located approximately 658 m from the trail head (herein termed the 18 m Ridge); 2) a lowland swale approximately 900 m wide (between 18 m Ridge and a 12 m high ridge to the west); 3) a 12 m ridge located approximately 2.1 km from the trail head (herein termed the 12 m Ridge); 4) another lowland swale approximately 1.3 km wide between 12 m Ridge and Six-Pack Pond to the west; 5) Six-Pack Pond located in the lowland area between 12 m Ridge and Long Lake Ridge, approximately 4 km from the trail head; and 6) Long Lake Ridge, located approximately 4.6 km from the trail head, which has two crests, and is approximately 700 m wide. Numerous banana holes occur in the swale regions along the trail and several pit caves occur near the crest of 12 m Ridge. The profile described above is depicted in Figure 2.

Analysis of the sixty thin sections from the Hard Bargain area reveals a distinctive pattern. Most of the rocks along the Hard Bargain Trail are composed largely of ooids, but in some regions they are composed of peloidal and bioclastic grains. Large amounts of sparite and micrite are found in some samples. These materials are believed to be recrystallization products . In the case of the sparite, some is cement, but much was produced by recrystallization in phreatic fresh water. Abundant micrite found in some samples is surface micritization and does not reflect a primary mud origin. Point count data for the sixty Hard Bargain Trail thin sections is summarized in Table 1. The pattern of ooid-dominated rocks observed along the trail is as follows: 1) high percentages of ooids occur at the top of 18 m Ridge and in the swale between 18 m Ridge and 12 m Ridge, 2) substantial amounts (>50%) of ooids from the crest and the east-facing side of 12 m Ridge, 3) high percentages of ooids in the swale region between 12 m Ridge and Long Lake Ridge, and 4) at the top and upper portions of both the east- and west-facing sides of Long Lake Ridge. Figure 3 shows the distribution of oolitic rocks observed along the Hard Bargain Trail.

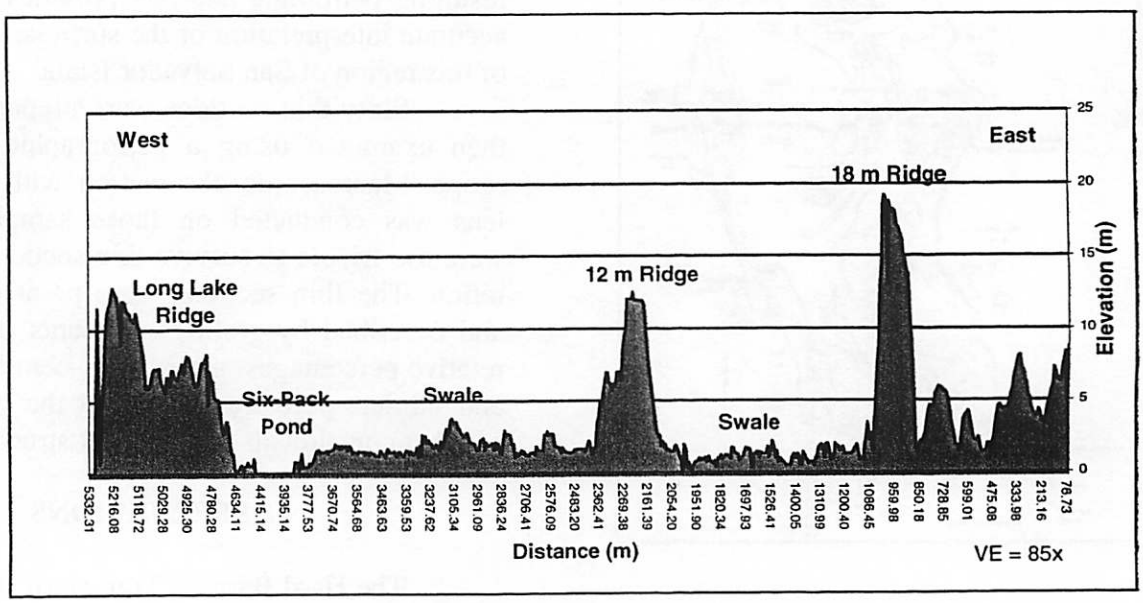

Figure 2. Geographic profile of the Hard Bargain Trail.

Station # or Sample Name	Distance (m)	Elevation (m)	Classification	% spar	% micrite	% inter-particle porosity	% intra-particle porosity	% total primary porosity	% vuggy porosity	% moldic porosity	% total secondary porosity	% calcite	% pyrobitumen	% blackrock	real tolerant	other
1	76.73	5.69														
SSHHB01	76.73	5.00	oolde/blocklosts - hand sample													
SSHHB02	145.00	7.00	sparite	0.38	0.08	0.52	0.00	0.52	0.01	0.01	0.02	0.01	0.01	0.02	0.00	0.03
SSHHB03	487.10	2.00	oopelsparite	0.08	0.02	0.23	0.00	0.23	0.01	0.07	0.08	0.42	0.12	0.02	0.00	0.06
SSHHB03A	487.20	2.00	oosparite	0.36	0.15	0.21	0.00	0.21	0.01	0.07	0.08	0.19	0.02	0.01	present	present
SSHHB03B	658.00	1.40	sparite	0.65	0.21	0.01	0.00	0.01	0.01	0.12	0.13	0.00	0.01	0.01	present	0.03
SSHHB04	948.00	17.00	oosparite	0.47	0.01	0.09	0.06	0.15	0.01	0.01	0.02	0.38	0.01	0.02	present	0.00
SSHHB05	1000.00	13.00	biopelmicrite	0.08	0.57	0.01	0.03	0.04	0.09	0.01	0.10	0.01	0.06	0.16	0.00	0.01
SSHHB06	1200.10	1.30	oopelsparite	0.11	0.09	0.13	0.04	0.17	0.01	0.11	0.12	0.28	0.22	0.02	0.00	0.00
SSHHB07A	1200.20	1.30	oolds - hand sample													
SSHHB07B	1200.30	1.30	oolds - hand sample													
SSHHB07C	1200.40	1.30	micrite	0.17	0.74	0.01	0.00	0.01	0.09	0.01	0.10	0.01	0.01	0.02	present	present
SSHHB07D	1200.50	1.30	pelagemicrite	0.17	0.37	0.01	0.05	0.06	0.01	0.22	0.23	0.09	0.10	0.01	0.00	0.00
SSHHB07E	1250.00	2.00	oopelsparite	0.27	0.01	0.16	0.02	0.18	0.01	0.09	0.10	0.28	0.18	0.01	0.00	0.00
SSHHB08	1300.00	1.00	oosparite	0.50	0.03	0.01	0.09	0.10	0.13	0.01	0.14	0.21	0.01	0.02	present	0.04
SSHHB09	1300.50	1.80	oomicrite	0.01	0.55	0.01	0.08	0.09	0.13	0.01	0.14	0.17	0.04	0.02	0.00	0.01
SSHHB10	1400.01	1.40	oopelsparite	0.31	0.01	0.23	0.05	0.28	0.02	0.01	0.03	0.27	0.10	0.02	0.00	0.00
SSHHB11	1400.02	0.50	oosparite	0.24	0.05	0.16	0.00	0.16	0.01	0.01	0.02	0.48	0.07	0.01	0.00	0.00
SSHHB12	1400.03	0.50	oopelsparite	0.40	0.01	0.13	0.02	0.15	0.03	0.01	0.04	0.29	0.12	0.02	present	0.02
SSHHB13	1400.04	1.25	oopelsparite	0.14	0.02	0.14	0.09	0.23	0.01	0.07	0.08	0.30	0.22	0.02	present	0.00
SSHHB14	1400.05	1.25	oolds - hand sample													
SSHHB15	1500.00	0.70	oolds - hand sample													
SSHHB16	1500.50	1.50	sparite	0.46	0.01	0.28	0.00	0.28	0.23	0.01	0.24	0.01	0.03	0.01	0.00	0.00
SSHHB17	1600.00	1.30	oolds - hand sample													
SSHHB18A	1600.50	1.30	oopelsparite	0.23	0.03	0.14	0.06	0.20	0.01	0.01	0.02	0.43	0.08	0.02	0.00	0.02
SSHHB18B	1700.00	1.70	oosparite	0.38	0.01	0.11	0.03	0.14	0.04	0.01	0.05	0.43	0.01	0.01	0.00	0.03
SSHHB19	1800.00	1.10	oolds - hand sample													
SSHHB20	1900.00	1.10	oopelsparite	0.30	0.01	0.23	0.04	0.27	0.01	0.01	0.02	0.22	0.18	0.03	0.00	0.00
SSHHB21	1900.01	0.70	oolds - hand sample													
SSHHB22	1900.00	0.70	oopelsparite	0.22	0.01	0.24	0.06	0.30	0.02	0.01	0.03	0.37	0.09	0.01	0.00	0.01
SSHHB23	1970.00	0.70	flowstone - hand sample													
SSHHB24	2000.00	1.60	oolds - hand sample													
SSHHB25	2000.50	1.60	oopelsparite	0.30	0.06	0.20	0.00	0.20	0.02	0.01	0.03	0.36	0.06	0.01	0.00	0.00
SSHHB26	2100.00	1.60	pelcosparite	0.29	0.01	0.08	0.06	0.14	0.02	0.01	0.03	0.28	0.29	0.01	0.00	0.00
SSHHB27	2100.50	2.60	oolds - hand sample													
SSHHB28	2200.00	12.00	oolds - hand sample													
SSHHB29	2300.50	7.00	pelsparite	0.24	0.01	0.17	0.06	0.23	0.01	0.01	0.02	0.01	0.48	0.05	0.00	0.00
SSHHB30	2300.60	7.00	biosparite	0.83	0.01	0.01	0.00	0.01	0.11	0.01	0.12	0.01	0.01	0.08	0.00	0.00
SSHHB31	2500.01	1.40	oolds - hand sample													
SSHHB32A	2500.02	1.40	oosparite	0.27	0.11	0.03	0.05	0.08	0.21	0.01	0.22	0.24	0.03	0.02	0.00	0.00
SSHHB32B	2900.03	1.40	oosparite	0.45	0.05	0.01	0.04	0.05	0.12	0.01	0.13	0.30	0.03	0.02	present	0.00
SSHHB33	2900.04	2.60	micrite	0.03	0.88	0.01	0.00	0.01	0.09	0.01	0.10	0.01	0.01	0.01	0.00	0.00
SSHHB34	2900.05	1.40	oosparite	0.55	0.24	0.01	0.00	0.01	0.09	0.01	0.10	0.11	0.01	0.02	present	0.02
SSHHB35	2700.00	1.40	oosparite	0.05	0.69	0.01	0.03	0.04	0.15	0.01	0.16	0.05	0.01	0.01	0.00	0.00
SSHHB36	2700.01	1.40	micrite	0.19	0.01	0.19	0.07	0.26	0.01	0.07	0.08	0.45	0.02	0.01	present	0.01
SSHHB37	2800.00	2.00	oosparite													
SSHHB38	2800.50	2.60	oolds - hand sample													
SSHHB39	2900.00	2.10	oosparite	0.45	0.14	0.01	0.02	0.03	0.11	0.01	0.12	0.23	0.04	0.02	present	0.00
SSHHB40	2900.50	2.00	oosparite	0.33	0.20	0.01	0.04	0.05	0.25	0.01	0.26	0.15	0.03	0.01	present	0.01
SSHHB41	2950.00	2.30	oosparite	0.21	0.05	0.11	0.07	0.18	0.01	0.01	0.02	0.50	0.06	0.01	0.00	0.00
SSHHB42	3000.00	2.10	oosparite	0.27	0.01	0.12	0.03	0.15	0.05	0.01	0.06	0.42	0.04	0.01	present	0.02
SSHHB43	3200.00	2.20	oosparite	0.20	0.01	0.26	0.06	0.32	0.01	0.01	0.02	0.42	0.06	0.01	0.00	0.00
SSHHB44	3300.00	1.20	oosparite	0.52	0.01	0.11	0.04	0.15	0.10	0.02	0.12	0.14	0.03	0.02	present	0.03
SSHHB45A	3400.00	1.50	oolds - hand sample													
SSHHB45B	3400.00	1.50	oomicrite	0.02	0.39	0.11	0.06	0.17	0.08	0.01	0.09	0.31	0.03	0.01	present	0.01
SSHHB46	3500.00	1.20	sparite	0.58	0.01	0.01	0.00	0.01	0.40	0.00	0.40	0.01	0.01	0.02	present	0.02
SSHHB47	3500.30	1.40	oosparite	0.41	0.08	0.01	0.07	0.08	0.09	0.01	0.10	0.28	0.02	0.02	present	0.01
SSHHB48	3500.80	1.40	oolds - hand sample													
SSHHB49	3600.00	1.40	oosparite	0.22	0.01	0.24	0.00	0.24	0.01	0.01	0.02	0.45	0.06	0.01	present	0.03
SSHHB50	3650.00	1.70	oolds - hand sample													
SSHHB51	3700.00	1.60	oosparite	0.42	0.01	0.03	0.04	0.07	0.19	0.01	0.20	0.25	0.05	0.02	present	0.02
SSHHB52	3700.01	1.40	oosparite	0.47	0.01	0.09	0.04	0.13	0.07	0.01	0.08	0.27	0.05	0.02	present	0.01
SSHHB53	3800.00	1.40	oosparite	0.33	0.03	0.15	0.06	0.21	0.04	0.02	0.06	0.30	0.06	0.01	present	0.01
SSHHB54	3800.30	0.80	oopelsparite	0.27	0.01	0.19	0.03	0.22	0.01	0.01	0.02	0.42	0.09	0.01	0.00	0.00
SSHHB55	3800.80	0.05	oosparite	0.22	0.01	0.22	0.14	0.36	0.01	0.01	0.02	0.36	0.05	0.01	0.00	0.01
SSHHB56	4000.00	0.50	oopelsparite	0.19	0.01	0.01	0.27	0.28	0.01	0.01	0.02	0.29	0.17	0.05	0.00	0.03
SSHHB57	4000.30	0.50	biopelsparite	0.32	0.22	0.03	0.03	0.06	0.12	0.01	0.13	0.03	0.12	0.16	0.00	0.00
SSHHB58	4000.00	4.80	oosparite	0.23	0.01	0.27	0.03	0.30	0.01	0.01	0.02	0.38	0.06	0.02	present	0.02
SSHHB59	4970.00	7.00	oosparite	0.27	0.01	0.22	0.03	0.25	0.01	0.01	0.02	0.37	0.06	0.02	present	0.01
SSHHB60	5100.00	6.00	oolds - hand sample													
SSHHB61	5200.00	9.00	oopelsparite	0.34	0.01	0.18	0.00	0.18	0.05	0.01	0.06	0.34	0.08	0.01	0.00	0.01
SSHHB62	5200.30	10.70	micrite	0.01	0.73	0.01	0.00	0.01	0.22	0.02	0.24	0.01	0.02	0.01	present	0.01
SSHHB63	5200.60	12.00	oosparite	0.39	0.01	0.14	0.00	0.14	0.04	0.01	0.05	0.35	0.05	0.02	present	0.01
SSHHB64	5300.00	11.50	oopelsparite	0.27	0.01	0.23	0.00	0.23	0.01	0.01	0.02	0.38	0.09	0.03	present	0.00
SSHHB65	5300.30	8.50	oolds - hand sample													
SSHHB66	5300.50	9.03	oopelsparite	0.29	0.04	0.10	0.08	0.16	0.10	0.01	0.11	0.31	0.12	0.02	present	0.01
SSHHB67	5300.60	9.03	oopelsparite	0.33	0.01	0.11	0.06	0.17	0.14	0.03	0.17	0.23	0.09	0.01	0.00	0.01
565	5302.31	0.03														
SSHHBAA	PIT CAVE		pelbiosparite	0.35	0.00	0.00	0.00	0.00	0.00	0.00	0.00	0.00	0.47	0.18	0.00	0.00
SSHHBBB	PIT CAVE		pelbiosparite	0.00	0.00	0.33	0.06	0.00	0.00	0.00	0.00	0.00	0.51	0.11	0.00	0.00
SSHHBCC	PIT CAVE		pelbiosparite	0.20	0.00	0.12	0.13	0.00	0.00	0.08	0.00	0.00	0.36	0.11	0.00	0.00
SSHHBDD	PIT CAVE		pelbiosparite	0.22	0.09	0.00	0.08	0.00	0.08	0.00	0.00	0.00	0.39	0.14	0.00	0.00

Table 1. Hard Bargain sample data.

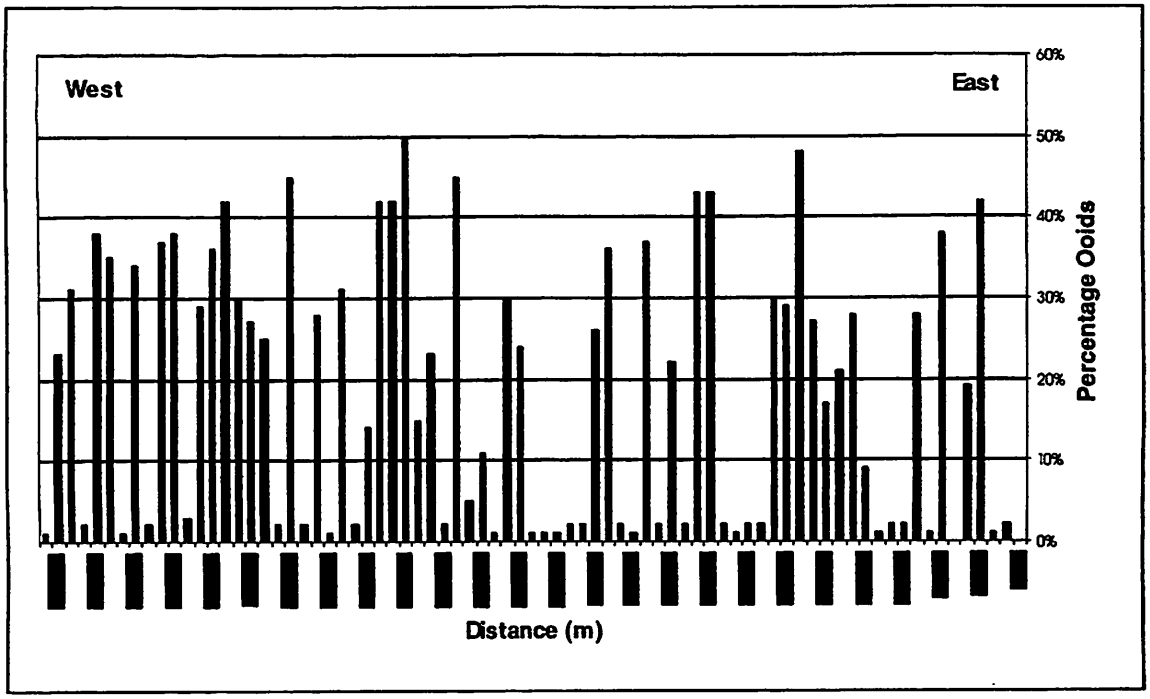

Figure 3. Ooid percentage along the length of the Hard Bargain Trail.

The greatest peloidal content is observed in rocks from the swale between 18 m Ridge and 12 m Ridge, particularly within 600 m of the east-facing side of 12 m Ridge. Peloids occur in varying percentages, but in those rocks, the ooid content is generally greater than that of the peloids. Significant peloidal content is also observed in rocks from the west-facing side of 12 m Ridge. Figure 4 shows the distribution of peloidal rocks observed along the Hard Bargain Trail.

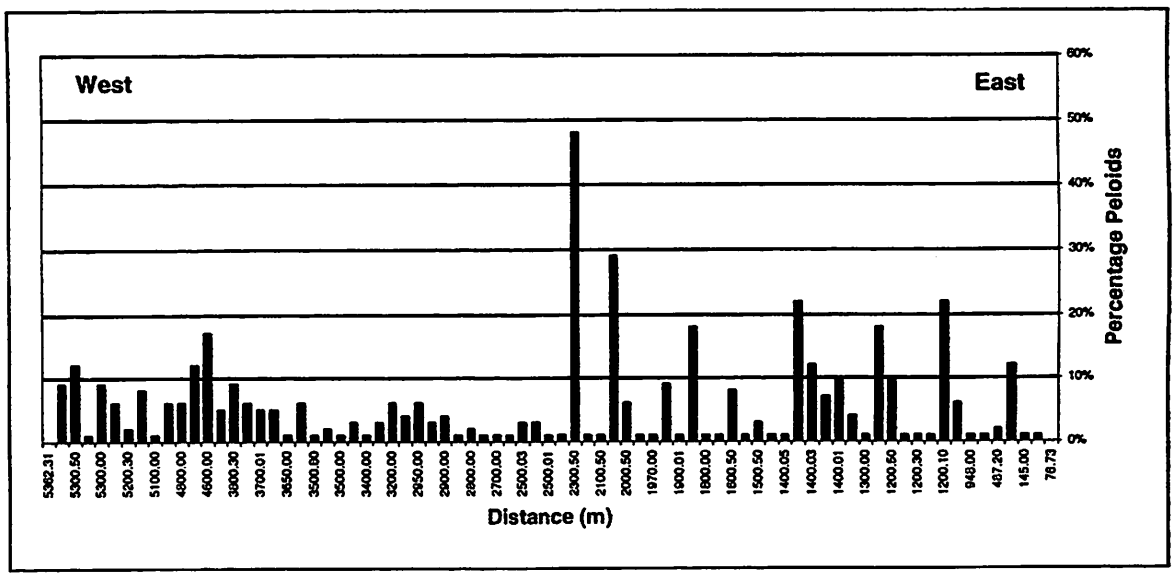

Figure 4. Peloid percentage along the length of the Hard Bargain Trail.

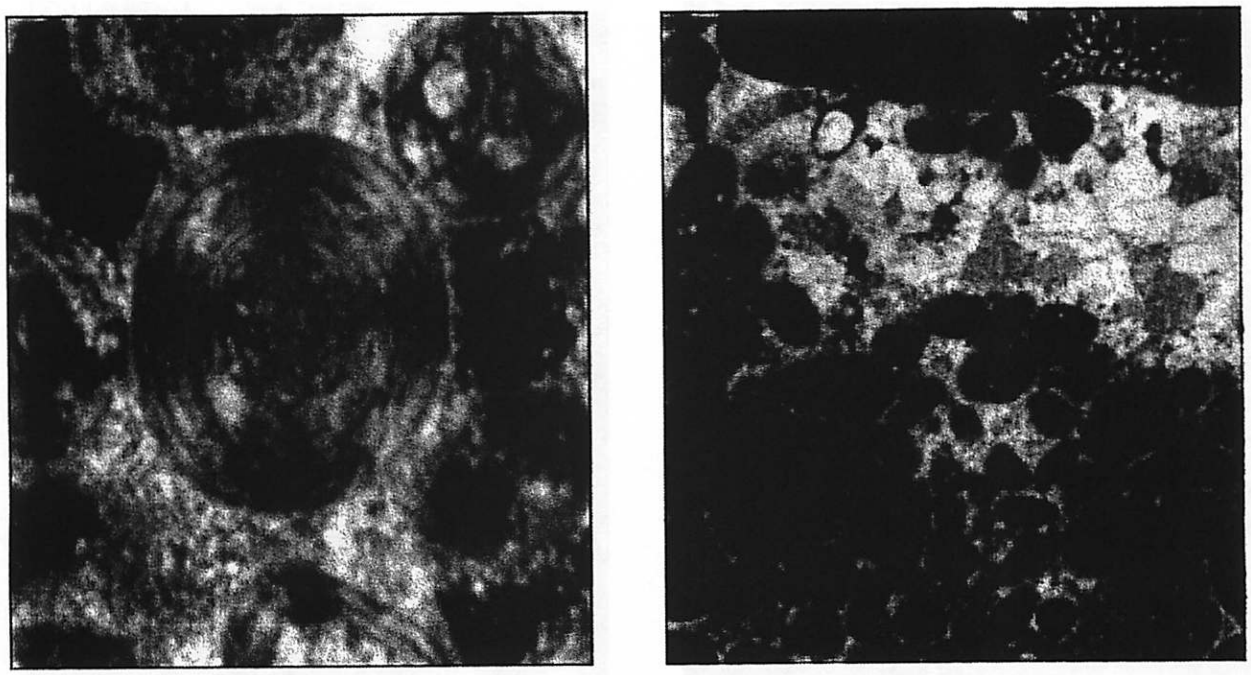

A. B.

Figure 5. A) Ooid. (magnification = 70x) B) Peloids typical of the Hard Bargain Trail samples. (magnification = 28x)

Figures 5A and 5B are photomicrographs of ooid and peloid allochems observed in samples from the trail. Rocks with a significant bioclastic component consisting of algae, foraminifera, molluscs, and other skeletal fragments, are also observed, but they are much less common. These rocks occur: 1) along the west-facing side of 18 m Ridge, 2) on the west-facing side of 12 m Ridge, and 3) at the eastward base of Long Lake Ridge. Figure 6 shows the bioclastic rock distribution and Figures 7A and 7B show examples.

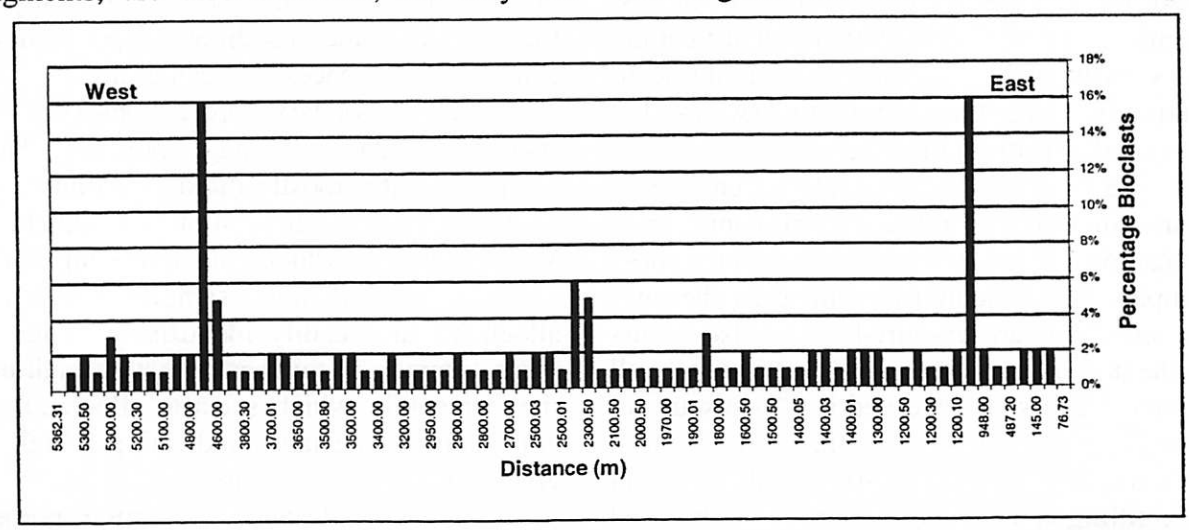

Figure 6. Bioclast percentage along the Hard Bargain Trail.

A.

B.

Figure 7. A) Foraminifera and coralline algae fragments. (magnification = 28x) B) Mollusc fragments. (magnification = 28x)

Several samples that have markedly low percentages of ooids are characterized by abundant sparry calcite and/or micrite, which obscures the ooids and other allochems. In some of the thin sections that are highly micritized, the outlines of ooids could still be distinguished, thus enabling their identification. Rocks with high percentages of micrite occur randomly along the trail in the swales, but they rarely occur on the ridges.

Samples with very high percentages of sparite most likely indicate significant recrystallization has occurred. As a result, these samples are difficult to characterize because the allochems are obscured. Spar also occurs as the dominant cement observed in nearly all samples. The spar observed is a meniscus cement that is concentrated at the grain contacts, indicating vadose cementation, and an equant pore filling cement more commonly observed in samples from the water-logged swales.

The primary porosity observed in the Hard Bargain thin sections consists largely of inter- and intraparticle porosity. Intraparticle porosity consists of naturally occurring spaces within allochems, such as the chambers of foraminifera tests. Interparticle porosity is formed at the time of sediment deposition, and consists of the spaces between grains.

The secondary porosity observed consists of moldic and vuggy porosity. These samples exhibit mostly moldic secondary porosity indicating dissolution of allochems. Vuggy porosity, which cuts across all fabrics, is observed in only a few samples in which the allochems are readily identifiable. Vugs are more common in thin sections with high micrite content in which specific allochems are not readily identifiable, indicating a high degree of diagenetic alteration.

Interparticle and intraparticle porosity is observed throughout the study area; but moldic and/or vuggy porosity is concentrated

in the lowland swale regions. This difference in diagenesis is most likely the result of greater exposure to meteoric water that frequently collects in the lows between the ridges.

DISCUSSION

Oolitic deposits on San Salvador Island have consistently yielded ages of approximately 125 ka, indicating deposition during the sea-level high stand associated with oxygen-isotope substage 5e (Grotto Beach Formation)(Carew and Mylroie, 1995). The transgressive-phase units deposited during that time have been shown to be especially high in ooid content, although there are appreciable percentages of peloids in some samples. A greater abundance of peloids is observed in some samples from the swale regions along the Hard Bargain Trail. Although this may possibly reflect original sediment composition, more likely the lower ooid content in these regions results from diagenetic alteration that destroyed the ooid structure and left a peloidal appearance. This greater diagenesis probably resulted from exposure to meteoric water that was observed to be ponded in these regions after storms.

Sample SS94HB05, located at the crest of 18 m Ridge, contains 38% ooids, with no observable bioclasts, whereas sample SS94HB06, located approximately 50 m from the crest on the west-facing side of the same ridge, contains 16% bioclasts, 6% peloids, and 1% ooids. The greater peloidal and bioclastic composition of sample SS94HB06 on the west-facing side of 18 m Ridge could represent a peloidal/bioclastic deposit that underlies an oolitic deposit represented by sample SS94HB05. In the field, no unconformity (paleosol) was observed between those units. This scenario might be explained by one of the following: 1) a paleosol on the lower bioclastic unit was eroded before deposition of the upper oolitic unit; 2) a paleosol is present between the two units, but it was not recognizable in the outcrops that were examined; or 3) no paleosol developed before deposition of the upper oolitic deposits, thus indicating only a change in sediment source during the same sea-level high stand.

Similar explanations might be offered for the presence of the bioclastic material observed on the west-facing side of 12 m Ridge. Sample SS94HB29 from the crest, and SS94HB28 at the base of the east-facing side of this ridge contain greater than 50% ooids (as observed in hand sample, not thin section). In contrast, samples SS94HB30 and SS94HB31, both collected approximately 100 m from the crest on the west-facing side of 12 m Ridge, contain no ooids, 42-49% peloids, and 5–6% bioclastic allochems, respectively. Further evidence that 12 m Ridge consists of two units is provided by investigation of samples obtained in a pit cave located near the crest of that ridge. At that location, a paleosol horizon can be observed in the outcrop, and all thin sections from below the paleosol contain abundant peloids (36-51%) and bioclasts (11-15%), but no ooids (0%).

These findings and interpretations are consistent with the work of Schwabe and others (1993) in which a petrologic study of ridges and caves at several localities, including Dixon Hill on San Salvador Island, was conducted. Those results consistently yielded data suggesting that the eolianite ridges consisted of an older, lower peloidal/bioclastic unit juxtaposed to and largely mantled by a younger oolitic unit deposited from the dominant wind direction, which varies according to position on the island. Schwabe and others (1993) also did not observe an unconformity (paleosol) between the two units at those locations. It should be noted that a paleosol between two eolianite units has only been recognized in quarries, road-cuts, cave walls, and cliffs, where there is near-vertical exposure.

The bioclastic rocks observed at the eastern base of Long Lake Ridge might also

document a younger oolitic unit that mantles an older eolianite. However, in this case, ooid-dominated deposits mantled the pre-existing peloidal/bioclastic eolianites from a northwesterly direction. The shapes of 18 m Ridge and 12 m Ridge indicate that they were formed by winds from the east. These eolianites have a transverse dune morphology, are curvilinear and convex to the west, and trend north-south with a steeper west-facing side. The observed distribution of rock types is consistent with a younger oolitic unit accreting onto the windward side of an older peloidal/bioclastic dune.

Long Lake Ridge has a morphology similar to that of 18 m Ridge and 12 m Ridge; however, Long Lake Ridge trends generally northeast-southwest with the steeper downwind side on the east. The occurrence of bioclastic rocks on the eastern side of this ridge is consistent with deposition of a younger oolitic unit that accreted onto the up-wind (northwest) side of an earlier dune. Interestingly, Clark and others (1989) showed that prevailing northwesterly winds from storms moving eastward off North America influenced sedimentation on the beaches on the west side of San Salvador, whereas prevailing easterly trade winds affected deposition on the east side of the island.

This conclusion was inferred from differences in the degree of variability in bioclasts, grain-size, and sorting observed in deposits from the eastern and western beaches. Deposits located on the west (lee) side were coarse-grained and had greater variability in grain sizes (poorer sorting). Those characteristics were correlated with deposition predominantly during storms from a northwesterly direction. In contrast, the deposits along the eastern side were predominantly fine- to medium-grained and well-sorted, indicating more consistent winds from the east.

Recent results of a paleomagnetic survey of the paleosol located in the swales of the Hard Bargain area (Panuska and others, this volume) indicate that this paleosol matches the Gaulin Cay magnetotype, and therefore the underlying rock is correlative to the Owl's Hole Formation. These palemagnetic data provide an independent means of confirming the petrographic observations reported here.

If the oolitic eolian deposits in the Hard Bargain area do indeed mantle a lower, older peloidal/bioclastic eolian unit, the stratigraphy there is consistent with the proposed stratigraphy of Carew and Mylroie (1985, 1995). The lower unit would represent the Owl's Hole Formation that was probably deposited during one or both of the sea-level high stands associated with oxygen-isotope stages 7 and/or 9, that occurred approximately 220 ka and 320 ka respectively. The upper ooid-dominated deposits are most likely the transgressive-phase of the Grotto Beach Formation that was deposited during oxygen-isotope substage 5e, approximately 125 ka. The relationship between these two units packaged within one dune ridge indicates that the use of morphostratigraphy as a tool for establishing the stratigraphic relationships of the inland eolianite ridges would be inaccurate. In addition, sampling only on the perimeter of the Hard Bargain region would also yield incomplete data.

CONCLUSION

This study represents the first detailed analysis of an interior landmass on San Salvador that is isolated from access by roads or lakes. Petrologic analyses of sixty samples collected along the Hard Bargain Trail reveal that the rocks located throughout the Hard Bargain region are predominantly oolitic. However, the presence of rocks with an abundance of other allochems (peloids and bioclasts), and their location along the trail (asymmetrically on ridges and in swale regions), indicates a specific pattern of deposition and/or diagenesis. It appears that older peloidal and bioclastic eolianites are mantled

by younger oolitic eolianites. Although no paleosol was visible between the units on the ridge slopes, a distinct paleosol was evident between a lower peloidal/bioclastic unit and an upper oolitic unit exposed in a pit cave near the top of 12 m Ridge. These findings are consistent with the earlier study of Schwabe and others (1993) that suggested the presence of younger (approximately 125 ka) ooid-dominated transgressive eolianites overlying older, peloidal/bioclastic units with no paleosol observed in between.

Cement types (sparite vs. micrite) vary among the samples collected from the trail. Micrite cement is more abundant in samples located in the swales, many containing peloidal allochems. The sparite cement observed in samples from the lowland swales is an equant pore filling sparite. The majority of ridge samples have a sparite cement displaying a meniscus texture, indicative of vadose development. Porosity also varies among the samples collected from the trail. The majority of secondary porosity is moldic or vuggy in the swales, which is probably indicative of a higher degree of dissolution due to greater exposure to meteoric water.

In conclusion, the variable compositions of the rocks observed along the Hard Bargain Trail indicate that rigorous sampling throughout the interior is needed to accurately assess the surficial geology of this region. Hearty and Kindler (1993) indicated that the entire Hard Bargain region consisted of rocks of the Grotto Beach Formation, based on morphostratigraphy and extrapolation of data obtained along the island's margins. This has proven to be inaccurate. In contrast, the geologic map of San Salvador drawn by Carew and Mylroie (1995) indicated only that the rocks of the Hard Bargain area were undifferentiated Pleistocene. The results of this study indicate that the rocks of the Hard Bargain area can now be assigned to two different stratigraphic units, the Grotto Beach Formation and the Owl's Hole Formation. This study further shows that detailed sampling of the interior of San Salvador Island can provide a better understanding of the surficial geology, and therefore a better understanding of the stratigraphy and the Quaternary history of the Bahamian islands.

ACKNOWLEDGMENTS

The authors would like to thank the entire staff of the Bahamian Field Station who provided facilities, lodging, and resources. Appreciation is extended to Dr. Bruce Panuska, of Mississippi State University, who risked life and limb to assist in this project. Thanks also to Dr. Larry Davis of the University of New Haven, and Dr. Paul Godfrey of the University of Massachusetts, for their assistance and guidance during the field seasons. Facilities for sample preparation were provided by the Geology Department at the College of Charleston. This project was partly funded by the Department of Geosciences at Mississippi State University.

The research presented in this paper would not have been possible were it not for the preliminary manual labor and reconnaissance work necessary to make the Hard Bargain region accessible. Thank you to all of the undergraduate and graduate students who assisted, especially Jonathan Harris, Marna Lehnert, Audra Moore, Brad Schmoll, Fred Toler, Jason Schleh, Steve Dudley, and Larry Smith.

REFERENCES

Carew, J.L., and Mylroie, J.E., 1985, The Pleistocene and Holocene stratigraphy of San Salvador Island, Bahamas, with reference to marine and terrestrial lithofacies at French Bay, *in* Curran, H.A., ed., Pleistocene and Holocene Carbonate Environments on San Salvador Island, Bahamas: Geological

Society of America, Orlando, Annual Meeting Field Trip Guidebook: Fort Lauderdale, Florida, CCFL Bahamian Field Station, p. 11-61.

Carew, J.L. and Mylroie, J.E., 1995, Depositional model and stratigraphy for the Quaternary geology of the Bahama islands, *in* Curran, H.A., and White, B., eds., Terrestrial and shallow marine geology of the Bahamas and Bermuda: Geological Society of America Special Paper 300, p. 5-32.

Carew, J.L., and Mylroie, J.E., 1997, Geology of the Bahamas, *in* Vacher, H.L., and Quinn, T.M., eds., Geology and hydrogeology of carbonate islands: Developments in Sedimentology, Elsevier Science Publishers, v. 54, p. 91-139.

Clark, D.D., Mylroie, J.E., and Carew, J.L., 1989, Texture and composition of Holocene beach sediment, San Salvador Island, *in* Mylroie, J.E., ed., Proceedings of the Fourth Symposium on the Geology of the Bahamas: Bahamian Field Station, San Salvador, Bahamas, p. 83-93.

Hearty, P.J., and Kindler, P., 1991, The geological evolution of San Salvador Island, Bahamas: Geological Society of America Abstracts with Programs, v. 23, no. 5, p. A225.

Hearty, P.J., and Kindler, P., 1992, The geological evolution of San Salvador Island, Bahamas: Abstracts and Program, Sixth Symposium on the Geology of the Bahamas: Bahamian Field Station, San Salvador, Bahamas, p. 11-12.

Hearty, P.J., and Kindler, P., 1993, New perspectives on Bahamian geology: San Salvador Island, Bahamas: Journal of Coastal Research, v. 9, p. 577-594.

Schwabe, S.J., Carew, J.L., and Mylroie, J.E., 1993, Petrology of Bahamian Pleistocene eolianites and flank margin caves: Implications for Late Quaternary island development, *in* White, B., ed., Proceedings of the Sixth Symposium on the Geology of the Bahamas: Port Charlotte, Florida, Bahamian Field Station, Ltd., p. 149-164.

Titus, R., 1980, Emergent facies patterns on San Salvador Island, Bahamas, *in* Gerace, D.T., ed., Field Guide to the Geology of San Salvador: Miami, Florida, CCFL Bahamian Field Station, p. 92-105.

Titus, R., 1987, Geomorphology, stratigraphy, and the Quaternary history of San Salvador, *in* Curran, H.A., ed., Proceedings of the Third Symposium on the Geology of the Bahamas: Fort Lauderdale, Florida, CCFL Bahamian Field Station, p. 155-164.